A reduced interface component mode synthesis method using coarse meshes

Citation for the original published paper (version of record):
Gibanica, M., Abrahamsson, T., Rixen, D. (2017). A reduced interface component mode synthesis method using coarse meshes. Procedia Engineering, 199: 348-353.
http://dx.doi.org/10.1016/j.proeng.2017.09.031

Available online at www.sciencedirect.com

ScienceDirect

Procedia Engineering 199 (2017) 348–353

Procedia Engineering

www.elsevier.com/locate/procedia

X International Conference on Structural Dynamics, EURODYN 2017

A reduced interface component mode synthesis method using coarse meshes

Mladen Gibanica[a,b,*], Thomas J. S. Abrahamsson[a], Daniel J. Rixen[c]

[a] *Chalmers University of Technology, Hörsalsvagen 7A, SE-41296 Göteborg, Sweden*
[b] *Volvo Car Corporation, SE-40531 Göteborg, Sweden*
[c] *Technical University of Munich, Boltzmannstraße 15, DE-85748 Garching, Germany*

Abstract

Component mode synthesis is a technique to simplify the analysis of complicated finite element models. A structure is split into substructures from which reduced order models can be generated and subsequently assembled. A model reduction performance gain can be limited if the component interfaces contain many degrees of freedom, which is often the case for high resolution models. In this paper a substructuring framework with interface reduction is presented. The method first splits a detailed model into substructures. The substructures' fine mesh is then coarsened on the internal region, while keeping the boundary mesh intact. Thereafter a Guyan reduction is performed on each coarse mesh substructure. The Guyan computations are cheap due to the reduced size of the linear equation system necessary to solve for the coarse mesh system. After synthesis of the statically reduced systems, a reduction basis for the interface degrees of freedom is computed. Thereafter a Craig-Bampton reduction is performed on each fine mesh substructure using projections with the reduced interface degrees of freedom and fixed interface modes. The method is verified on a dense mesh plate model consisting of two substructures.

Peer-review under responsibility of the organizing committee of EURODYN 2017.

Keywords: Substructuring; component mode synthesis; interface reduction; mesh coarsening

1. Introduction

Initial ideas for the component mode synthesis (CMS) method were first published by Hurty [1,2] and Gladwell [3]. These ideas were further developed by Guyan [4], resulting in the well known Guyan method for condensing the internal degrees of freedom (DOFs) to the boundary DOFs, and later extended by Craig and Bampton [5] as a substructuring method where the internal dynamics were also accounted for by including fixed interface modes in the reduction basis. The Guyan and Craig-Bampton (CB) methods are widely used in industry and are available in most finite element (FE) software. Throughout the years there have been many variations and advances made to the previously mentioned methods. For a historical review see [6].

* Corresponding author. Tel.: +46 31 772 10 00
E-mail address: mladen.gibanica@chalmers.se

1877-7058
Peer-review under responsibility of the organizing committee of EURODYN 2017.
10.1016/j.proeng.2017.09.031

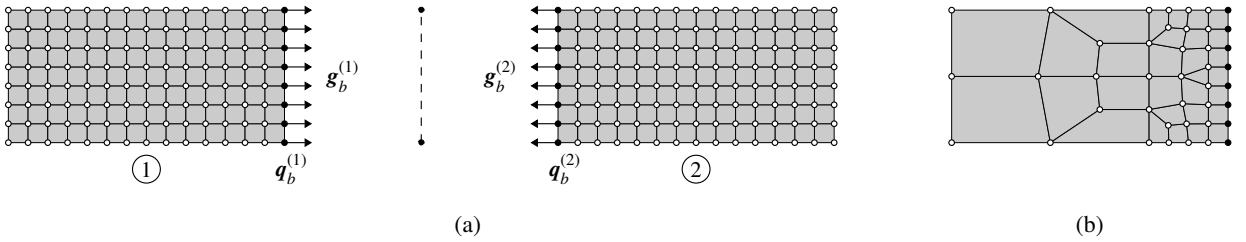

Fig. 1: (a) two identical substructures to be joined, and (b) a coarsened internal mesh of one substructure. Here ∘ denote internal nodes associated with $q_i^{(s)}$ and • denote boundary nodes associated with $q_b^{(s)}$. The arrows ⟶ denote boundary forces $g_b^{(s)}$ felt from neighbouring structures.

The CB reduction method relies on the formulation of a reduction basis consisting of static constraint modes and fixed interface normal modes. The static constraint modes are computed using Guyan reduction and are directly related to the number of boundary, or interface, DOFs. The numbers of fixed interface modes can be selected arbitrarily by the user to capture the dynamical range of interest. In applications where the fixed interface modes are small in comparison to the static constraint modes, or the FE model mesh is very dense with many boundary DOFs, the CB reduction efficiency decreases. Therefore, methods have been proposed to reduce the interface DOFs. The problem was first considered by Craig and Chang [7], where modal, Guyan and Ritz reduction methods were proposed. In [8] Balmès proposed a generalisation of the static constraint modes, simply denoted generalised interface DOFs. The generalised static constraint modes are defined as linear combinations of the static modes through a basis of interface deformations. The basis can be formed in various ways with the underlying assumption that it is representative of the actual displacements around the interfaces. For free and hybrid interface methods Tran [9] extended the interface reduction methods, with applications to cyclic symmetrical problems, and further extended the method for partial interface reduction [10], i.e. when some physical DOFs of the interface are kept out of reduction. In [11] Aoyama and Yagawa proposed that interface vibration modes for the CMS method be computed from local interface modes of connected substructures. Zhang, Castanier and Pierre noted in [12] that a static constraint mode is usually heavily localised to the surrounding of the associated interface DOF. Therefore, if internal DOFs experience negligible displacement, the corresponding static reduction basis elements can be set to zero, i.e. a filtering of elements less than a certain threshold was proposed. Other approaches to the interface reduction problem exist, such as the wave-based substructuring approach by Donders et al. [13]. For further methods see [6,14–16].

In this paper a simple methodology for fast interface reduction is presented. The Guyan reduction is made efficient through mesh coarsening, so that the size of the linear equation system in the Guyan reduction computations is considerably reduced. Results from an implementation of the method in MATLAB will be presented here. This paper is organized as follows. In Section 2 the theory behind the method is explained and in Section 3 the numerical results of the analysis of a plate with three holes and a high density mesh is shown. Further, in Section 4 the method is related to other interface reduction methods and in Section 5 the paper is concluded.

2. Theory

No notational differences for system matrices and vectors of the coarse and fine substructures are made here, rather it should be obvious from the context. The equations of motion (EOMs) for an undamped, linear mechanical system of some component (s) can be written as

$$\boldsymbol{M}^{(s)}\ddot{\boldsymbol{q}}^{(s)}(t) + \boldsymbol{K}^{(s)}\boldsymbol{q}^{(s)}(t) = \boldsymbol{f}^{(s)}(t) + \boldsymbol{g}^{(s)}(t) \tag{1}$$

where $\boldsymbol{M} \in \mathbb{R}^{n\times n}$ and $\boldsymbol{K} \in \mathbb{R}^{n\times n}$ represent the mass and stiffness matrices, respectively. Here $\boldsymbol{q} \in \mathbb{R}^{n\times 1}$ denote the displacement vector associated to the DOFs, $\boldsymbol{f} \in \mathbb{R}^{n\times 1}$ the external excitation force vector and $\boldsymbol{g} \in \mathbb{R}^{n\times 1}$ the interface force vector representing the counteracting forces from neighbouring structures, denoted boundary forces. The dot notation is adopted for time differentiation. Explicit time dependence (t), and substructure (s) notation is here on dropped for brevity. The derivations will be made for one substructure, but the procedure is identical for the other substructures and should be obvious from the presentation. The following treats the eigenproblem and therefore

$\boldsymbol{f}^{(s)} = \boldsymbol{0}$ in Eq. (1). It is now possible to partition the DOF vector in Eq. (1) into a boundary (or interface) set b and an internal set i, with n_b and n_i DOFs each. The EOMs from Eq. (1) can then be written as follows

$$\begin{bmatrix} \boldsymbol{M}_{bb} & \boldsymbol{M}_{bi} \\ \boldsymbol{M}_{ib} & \boldsymbol{M}_{ii} \end{bmatrix} \begin{bmatrix} \ddot{\boldsymbol{q}}_b \\ \ddot{\boldsymbol{q}}_i \end{bmatrix} + \begin{bmatrix} \boldsymbol{K}_{bb} & \boldsymbol{K}_{bi} \\ \boldsymbol{K}_{ib} & \boldsymbol{K}_{ii} \end{bmatrix} \begin{bmatrix} \boldsymbol{q}_b \\ \boldsymbol{q}_i \end{bmatrix} = \begin{bmatrix} \boldsymbol{g}_b \\ \boldsymbol{g}_i \end{bmatrix}. \tag{2}$$

Moreover, $\boldsymbol{g}_i^{(s)} = \boldsymbol{0}$, as neighbouring substructures do not affect the internal nodes of substructure (s). Two similar substructures to be assembled can be seen in Fig. 1a. In Fig. 1b a coarsened internal mesh of one substructure is shown, such that the coarse and fine meshes are conforming at the boundary nodes. Herein the case of two substructures coupled through one common interface is shown for simplicity, but the general case is easily implemented using the primal assembly formulation shown in [6,14]. For two substructures the compatibility condition states that $\boldsymbol{q}_b^{(1)} = \boldsymbol{q}_b^{(2)}$ and the equilibrium condition states that $\boldsymbol{g}_b^{(1)} + \boldsymbol{g}_b^{(2)} = 0$.

The first step in the substructuring procedure, apart from coarsening the fine mesh which is out of the scope of this paper but will briefly be mentioned in Section 5, is to statically condense the internal degrees of freedom using Guyan reduction [4,17,18] for the coarse mesh of each substructure.

$$\begin{bmatrix} \boldsymbol{q}_b \\ \boldsymbol{q}_i \end{bmatrix} = \begin{bmatrix} \boldsymbol{I} \\ -\boldsymbol{K}_{ii}^{-1}\boldsymbol{K}_{ib} \end{bmatrix} \boldsymbol{q}_b \triangleq \begin{bmatrix} \boldsymbol{I} \\ \boldsymbol{\Psi}_c \end{bmatrix} \boldsymbol{q}_b \triangleq \boldsymbol{R}_c \boldsymbol{q}_b \tag{3}$$

The EOMs in Eq. (1) can now be reduced for the coarse model, using the basis $\boldsymbol{R}_c$ such that $\boldsymbol{M}_c = \boldsymbol{R}_c^T \boldsymbol{M} \boldsymbol{R}_c$, $\boldsymbol{K}_c = \boldsymbol{R}_c^T \boldsymbol{K} \boldsymbol{R}_c$ and $\boldsymbol{g}_b = \boldsymbol{R}_c^T \boldsymbol{g}$, and the substructure assembly is then simply

$$\tilde{\boldsymbol{M}}_c \ddot{\boldsymbol{q}}_b + \tilde{\boldsymbol{K}}_c \boldsymbol{q}_b = \boldsymbol{0} \quad \text{with} \quad \tilde{\boldsymbol{M}}_c = \boldsymbol{M}_c^{(1)} + \boldsymbol{M}_c^{(2)} \quad \text{and} \quad \tilde{\boldsymbol{K}}_c = \boldsymbol{K}_c^{(1)} + \boldsymbol{K}_c^{(2)} \tag{4}$$

assuming for simplicity that the boundary DOFs have the same numbering on each side. Next the eigenvalue problem for the above system is solved for the eigenvalues $\boldsymbol{\Lambda} \in \mathbb{R}^{n_b \times n_b}$

$$\left(\tilde{\boldsymbol{M}}_c - \boldsymbol{\Lambda} \tilde{\boldsymbol{K}}_c \right) \boldsymbol{\Phi} = \boldsymbol{0} \tag{5}$$

where a partition of the eigenvector matrix $\boldsymbol{\Phi} \in \mathbb{R}^{n_b \times n_b}$ is used for interface reduction. Let $\boldsymbol{\Phi}_b \in \mathbb{R}^{n_b \times m_b}$ be that partition that includes the m_b lowest eigenfrequency modes of the assembled system. It is important to note that a major cost in building the reduced problem in Eq. (4) consists in computing the interface static constraint modes in Eq. (3) on which the system matrices are projected. In particular computing the internal DOFs from $-\boldsymbol{K}_{ii}^{-1}\boldsymbol{K}_{ib}$ requires solving n_b problems of dimension n_i. It is thus clear that using a coarse mesh to generate the interface modes can significantly reduce the computational cost.

From here on the fine mesh system matrices are considered. The reduction basis $\boldsymbol{\Phi}_b$ is used to reduce the interface DOFs of the fine mesh problem, using the same partitioning as in Eq. (2).

$$\begin{bmatrix} \boldsymbol{q}_b \\ \boldsymbol{q}_i \end{bmatrix} = \begin{bmatrix} \boldsymbol{\Phi}_b & \boldsymbol{0} \\ \boldsymbol{0} & \boldsymbol{I} \end{bmatrix} \begin{bmatrix} \boldsymbol{\eta}_b \\ \boldsymbol{q}_i \end{bmatrix} \triangleq \boldsymbol{T}_\eta \bar{\boldsymbol{q}} \tag{6}$$

Here $\boldsymbol{\eta}_b$ are the reduced interface DOFs. The transformation is applied to the fine mesh system in Eq. (1), without boundary forces, to find the static constraint modes.

$$\boldsymbol{M}_\eta \ddot{\bar{\boldsymbol{q}}} + \boldsymbol{K}_\eta \bar{\boldsymbol{q}} = \boldsymbol{0} \quad \text{with} \quad \boldsymbol{M}_\eta = \boldsymbol{T}_\eta^T \boldsymbol{M} \boldsymbol{T}_\eta = \begin{bmatrix} \boldsymbol{\Phi}_b^T \boldsymbol{M}_{bb} \boldsymbol{\Phi}_b & \boldsymbol{\Phi}_b^T \boldsymbol{M}_{bi} \\ \boldsymbol{M}_{ib} \boldsymbol{\Phi}_b & \boldsymbol{M}_{ii} \end{bmatrix} \quad \text{and} \quad \boldsymbol{K}_\eta = \boldsymbol{T}_\eta^T \boldsymbol{K} \boldsymbol{T}_\eta = \begin{bmatrix} \boldsymbol{\Phi}_b^T \boldsymbol{K}_{bb} \boldsymbol{\Phi}_b & \boldsymbol{\Phi}_b^T \boldsymbol{K}_{bi} \\ \boldsymbol{K}_{ib} \boldsymbol{\Phi}_b & \boldsymbol{K}_{ii} \end{bmatrix} \tag{7}$$

Now a Guyan reduction, as shown in Eq. (3), is performed for the reduced interface fine mesh system in Eq. (7) so that

$$\begin{bmatrix} \boldsymbol{\eta}_b \\ \boldsymbol{q}_i \end{bmatrix} = \begin{bmatrix} \boldsymbol{I} \\ -\boldsymbol{K}_{ii}^{-1}\boldsymbol{K}_{i\eta} \end{bmatrix} \boldsymbol{\eta}_b \triangleq \begin{bmatrix} \boldsymbol{I} \\ \boldsymbol{\Psi}_f \end{bmatrix} \boldsymbol{\eta}_b \triangleq \boldsymbol{R}_f \boldsymbol{\eta}_b \quad \text{with} \quad \boldsymbol{K}_{i\eta} = \boldsymbol{K}_{ib} \boldsymbol{\Phi}_b. \tag{8}$$

For the CB reduction a basis of fixed interface modes is also needed. This is acquired by solving a similar eigenvalue problem as in Eq. (5), but for $\boldsymbol{K}_{ii}$ and $\boldsymbol{M}_{ii}$ of the fine mesh, which are unaffected by the transformation $\boldsymbol{T}_\eta$ as seen in

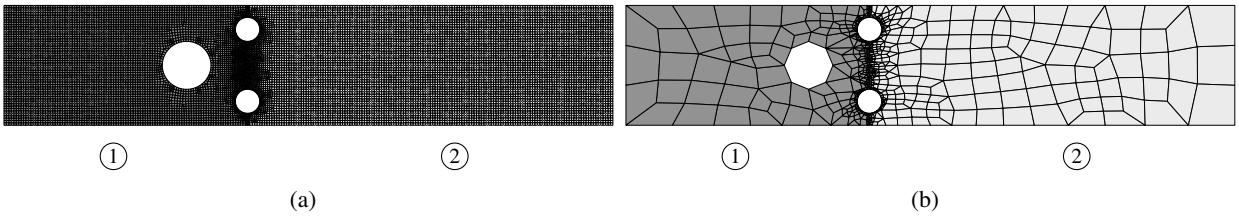

Fig. 2: (a) the two assembled fine mesh substructures considered, and (b) the same model, but with a coarsened internal mesh.

Eq. (7). From the eigenvector matrix a reduced number of modes m_i are selected as $\boldsymbol{\Phi}_i \in \mathbb{R}^{n_i \times m_i}$ with $m_i < n_i$. It is now possible to form the CB reduction basis, with $\boldsymbol{\eta}_i$ denoting the generalised internal DOFs.

$$\begin{bmatrix} \boldsymbol{q}_b \\ \boldsymbol{q}_i \end{bmatrix} = \boldsymbol{T}_\eta \boldsymbol{T}_b \boldsymbol{\eta} = \begin{bmatrix} \boldsymbol{\Phi}_b & \boldsymbol{0} \\ \boldsymbol{0} & \boldsymbol{I} \end{bmatrix} \begin{bmatrix} \boldsymbol{I} & \boldsymbol{0} \\ \boldsymbol{\Psi}_f & \boldsymbol{\Phi}_i \end{bmatrix} \begin{bmatrix} \boldsymbol{\eta}_b \\ \boldsymbol{\eta}_i \end{bmatrix} = \begin{bmatrix} \boldsymbol{\Phi}_b & \boldsymbol{0} \\ \boldsymbol{\Psi}_f & \boldsymbol{\Phi}_i \end{bmatrix} \begin{bmatrix} \boldsymbol{\eta}_b \\ \boldsymbol{\eta}_i \end{bmatrix} \triangleq \boldsymbol{T} \boldsymbol{\eta} \tag{9}$$

Here $\boldsymbol{T}_b$ is identified as the CB reduction basis [5] without reduced interfaces. The reduced fine mesh system is then

$$\bar{\boldsymbol{M}} \ddot{\boldsymbol{\eta}} + \bar{\boldsymbol{K}} \boldsymbol{\eta} = \bar{\boldsymbol{g}} \quad \text{with} \quad \bar{\boldsymbol{M}} = \boldsymbol{T}^T \boldsymbol{M} \boldsymbol{T} = \begin{bmatrix} \bar{\boldsymbol{M}}_{bb} & \bar{\boldsymbol{M}}_{bi} \\ \bar{\boldsymbol{M}}_{ib} & \bar{\boldsymbol{M}}_{ii} \end{bmatrix}, \quad \bar{\boldsymbol{K}} = \boldsymbol{T}^T \boldsymbol{K} \boldsymbol{T} = \begin{bmatrix} \bar{\boldsymbol{K}}_{bb} & \bar{\boldsymbol{K}}_{bi} \\ \bar{\boldsymbol{K}}_{ib} & \bar{\boldsymbol{K}}_{ii} \end{bmatrix} \quad \text{and} \quad \bar{\boldsymbol{g}} = \boldsymbol{T}^T \boldsymbol{g} = \begin{bmatrix} \boldsymbol{\Phi}_b^T \boldsymbol{g}_b \\ \boldsymbol{0} \end{bmatrix} \tag{10}$$

and the assembly of the two substructures can be written as follows, with $\bar{\boldsymbol{g}}^{(1)} + \bar{\boldsymbol{g}}^{(2)} = \boldsymbol{\Phi}_b (\boldsymbol{g}_b^{(1)} + \boldsymbol{g}_b^{(2)}) = \boldsymbol{0}$.

$$\tilde{\boldsymbol{M}} \ddot{\boldsymbol{x}} + \tilde{\boldsymbol{K}} \boldsymbol{x} = \boldsymbol{0} \quad \text{with} \quad \tilde{\boldsymbol{M}} = \begin{bmatrix} \bar{\boldsymbol{M}}_{bb}^{(1)} + \bar{\boldsymbol{M}}_{bb}^{(2)} & \bar{\boldsymbol{M}}_{bi}^{(1)} & \bar{\boldsymbol{M}}_{bi}^{(2)} \\ \bar{\boldsymbol{M}}_{ib}^{(1)} & \bar{\boldsymbol{M}}_{ii}^{(1)} & 0 \\ \bar{\boldsymbol{M}}_{ib}^{(2)} & 0 & \bar{\boldsymbol{M}}_{ii}^{(2)} \end{bmatrix}, \quad \tilde{\boldsymbol{K}} = \begin{bmatrix} \bar{\boldsymbol{K}}_{bb}^{(1)} + \bar{\boldsymbol{K}}_{bb}^{(2)} & \bar{\boldsymbol{K}}_{bi}^{(1)} & \bar{\boldsymbol{K}}_{bi}^{(2)} \\ \bar{\boldsymbol{K}}_{ib}^{(1)} & \bar{\boldsymbol{K}}_{ii}^{(1)} & 0 \\ \bar{\boldsymbol{K}}_{ib}^{(2)} & 0 & \bar{\boldsymbol{K}}_{ii}^{(2)} \end{bmatrix} \quad \text{and} \quad \boldsymbol{x} = \begin{bmatrix} \boldsymbol{\eta}_b \\ \boldsymbol{\eta}_i^{(1)} \\ \boldsymbol{\eta}_i^{(2)} \end{bmatrix} \tag{11}$$

It should be noted that $\boldsymbol{K}_{ii}^{(s)}$ is diagonal as in the normal CB procedure, but $\boldsymbol{K}_{ib}^{(s)}$ is in general not zero. This renders the solution of the reduced problem slightly less efficient, which is not an issue for small systems. The proposed method computes two Guyan reductions where the first one is efficient due to the coarse mesh, and the second is efficient due to the reduced number of problems to solve, i.e. equal to the number of reduced interface DOFs m_b.

3. Application

A plate of thickness 0.01 m consisting of two parts, shown in Fig. 2, is considered. The model is created using Femap with NX Nastran version 10.3. Four noded Mindlin-Reissner plate elements are used. The left part in Fig. 2a represent a steel plate (E = 210 GPa, $\nu = 0.30$, $\rho = 7850$ kg/m^3) with length 2 m and height 1 m with 5298 nodes, and the right part in Fig. 2a represent an aluminium plate (E = 70 GPa, $\nu = 0.30$, $\rho = 2100$ kg/m^3) with length 3 m and height 1 m with 8124 nodes. The interface region consists of 63 nodes. Two holes with diameter 0.2 m exist at the boundary of the parts, and one additional central hole with diameter 0.4 m is located in the steel part 0.3 m from the interface. A coarsened internal mesh for the two parts is shown in Fig. 2b. It can be noted that the boundary DOFs are unchanged. In generating the static constraint modes this region is most important, and hence a computationally efficient interface reduction of good quality is achieved.

In Table 1 the mean simulation times for four different cases can be seen. Each case is run five times due to variations between identical runs. The baseline simulation is performed with NX Nastran for 200 modes. It can be seen that the same solution with MATLAB took 1.36 times longer. The proposed method, with 22 generalised interface modes and 110 fixed interface modes, for each substructure, so that in total 242 modes were considered, is equal to the baseline simulation. For comparison a simulation was performed, using the fine mesh in creating the interface reduction basis, which took 1.64 times longer than the baseline simulation. It should be noted that for the fine mesh interface reduction it is only necessary to compute the Guyan reduction basis once because of the relation $\boldsymbol{\Psi}_f = \boldsymbol{\Psi}_c \boldsymbol{\Phi}_b$. Further, it should be noted that no parallelisation is performed here. Because of the independence of the substructures, Eqs. (6) to (10) can be performed in parallel. The proposed method could in this case have a theoretical

Table 1: Mean simulation times for 5 simulations, relative to the mean simulation time of Nastran NX. Interface denotes creation of the interface reduction basis without mesh coarsening. Substructure ({1,2}) denotes the generation of the Craig-Bampton system of the fine mesh system.

Simulation stage	Fine interface reduction	Coarse interface reduction	Full system (MATLAB)	Full system (Nastran NX)
Interface, Eqs. (3) to (5)	0.90	0.03	-	-
Substructure (1), Eqs. (6) to (11)	0.29	0.38	-	-
Substructure (2), Eqs. (6) to (11)	0.45	0.57	-	-
Total solution	1.64	0.99	1.36	1.00

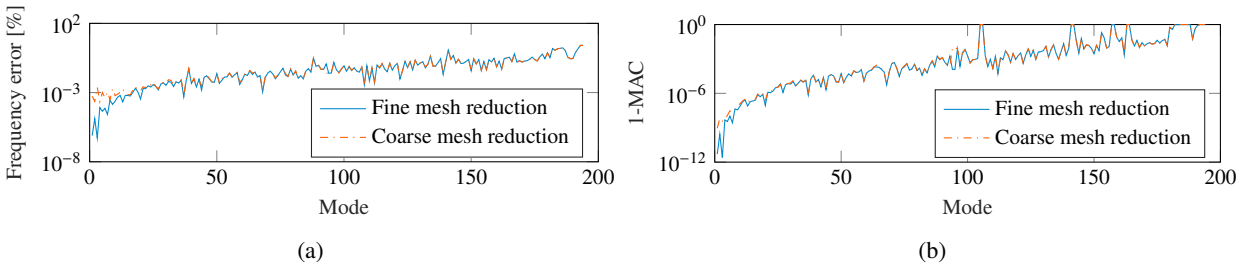

Fig. 3: (a) the relative eigenfrequency difference for the fine and coarse interface reduction relative the true system, and (b) the diagonal $1 - MAC$ values relative the true system.

simulation time 0.6 times the baseline simulation. It should be pointed out that the proposed method is implemented in MATLAB, which is shown to be 1.36 times slower compared to NX Nastran. Therefore, an implementation using NX Nastran's eigenvalue solver would probably show a significant decrease in computational time. Further, the method could be extended in a multilevel scheme where the substructures are further split into smaller substructures and the simulations performed in parallel. It should also be noted that mesh coarsening is not included in the simulation times. However, it has been observed that creating coarse surface meshes is negligible in time, compared to the CB reduction basis computations. In Table 1 the simulation time for the assembly and eigenvalue solution of the final reduced system is not reported due to negligible time relative the total simulation time.

The proposed method is an approximation and therefore introduces errors. In Fig. 3a the eigenfrequency error relative the full system for solutions with fine and coarse mesh interface reduction is shown, considering only flexible modes up to mode 200. It can be seen that the differences are negligible. For the coarse mesh interface reduction the maximum relative error introduced for the eigenfrequencies is 2.596%. In comparison, using the fine mesh for interface reduction introduces a maximum relative error of 2.592%. Hence, there is no gain in using the fine mesh for interface reduction, and considering the cost is not justifiable. The modeshape approximation is more crude. It is verified with the modal assurance criterion (MAC) [19] for all DOFs, and found that good correlation relative the full system with MAC correlations larger than 0.98 up to flexible mode 104 is achieved. The diagonal MAC values for the two cases can be seen in Fig. 3b. After flexible mode 104 there are occasional mode shifts, indicated by peaks in Fig. 3b, but the overall correlation is good up to mode 179. However, as for the eigenfrequencies, very little is gained in modeshape correlation by using the fine mesh for interface reduction.

4. Similarities to different methods

Similarities between the proposed idea and the previously mentioned methods exist. In this paper the idea of modal reduction of the interfaces as proposed by Craig and Chang in [7], in conjunction with mesh coarsening, is used. The idea is similar to what Balmès [8] proposed, where a local model is solved, consisting of only a few elements surrounding the interfaces. A suggestion was made towards using a full model, and then applying Guyan reduction to it. This is utilised in this paper, but made efficient through a coarsened internal mesh of the connecting substructures. Further, Zhang, Castanier and Pierre had noted in [12] that only the region near the interfaces were important for the static constraint modes, which is in some sense also utilised here, in that the coarse mesh is detailed near the interface and coarsened further away from the interfaces, where detailed knowledge about the static behaviour

is not necessary. Thus the mesh coarsening alleviates the need for filtering the static reduction matrix. The advantage of the proposed method is that the interface reduction basis is accurate and produces conforming interfaces as it is computed from the assembled substructures. It is also simple to implement as no re-modelling is necessary, only mesh coarsening which can be automated, and no additional steps not already existing in software are necessary.

5. Conclusion

An interface reduction method is presented, using coarse substructure meshes to generate statically condensed systems that are assembled. The Guyan computations are therefore very efficient in that linear systems of much smaller size need to be solved. The eigenvector basis of this assembled system is truncated such that the fine mesh boundary can be reduced. The normal Craig-Bampton procedure is then employed. It has been shown, for a plate structure divided into two substructures, that the interface reduction is very fast, and that a good approximation of the interface behaviour is achieved for eigenfrequencies, and a more crude approximation for modeshapes. It is also shown that there is no significant accuracy gain in using the fine mesh in generating the interface reduction basis, and that it is much slower. In fact it is possible to rival the Lanczos solver in NX Nastran with the proposed approach, given that the mesh coarsening can be automated and made efficient, which is assumed in this paper. The method could be further optimised in a multi-level substructuring approach. A possibility is also to perform a static condensation on a subset of all nodes in the fine mesh, alleviating the need for a coarse mesh. This is the subject of future work. The proposed method is reduced in efficiency, as are all interface reduction methods, when the interface region is coarse or small, i.e. when there is no gain in reducing the interfaces.

Acknowledgements

Volvo Car Corporation is gratefully acknowledged for providing the funding for this paper.

References

[1] W. C. Hurty, Vibrations of Structural Systems by Component Mode Synthesis, Journal of the Engineering Mechanics Division 86 (1960) 51–70.
[2] W. C. Hurty, Dynamic analysis of structural systems using component modes, AIAA Journal 3 (1965) 678–685.
[3] G. M. L. Gladwell, Branch mode analysis of vibrating systems, Journal of Sound and Vibration 1 (1964) 41–59.
[4] R. J. Guyan, Reduction of stiffness and mass matrices, AIAA Journal 3 (1965) 380–380.
[5] M. C. C. Bampton, R. R. Craig, Jr., Coupling of substructures for dynamic analyses, AIAA Journal 6 (1968) 1313–1319.
[6] D. D. Klerk, D. J. Rixen, S. N. Voormeeren, General Framework for Dynamic Substructuring: History, Review and Classification of Techniques, AIAA Journal 46 (2008) 1169–1181.
[7] R. R. J. Craig, C. J. Chang, Substructure coupling for dynamic analysis and testing, Technical Report, 1977. URL: http://ntrs.nasa.gov/search.jsp?R=19770010568.
[8] E. Balmès, Use of generalized interface degrees of freedom in component mode synthesis, in: Proceedings of the 14th IMAC, 1996.
[9] D. M. Tran, Component mode synthesis methods using interface modes. Application to structures with cyclic symmetry, Computers & Structures 79 (2001) 209–222.
[10] D.-M. Tran, Component mode synthesis methods using partial interface modes: Application to tuned and mistuned structures with cyclic symmetry, Computers & Structures 87 (2009) 1141–1153.
[11] Y. Aoyama, G. Yagawa, Component mode synthesis for large-scale structural eigenanalysis, Computers & Structures 79 (2001) 605–615.
[12] G. Zhang, M. P. Castanier, C. Pierre, Efficient Component Mode Synthesis With a New Interface Reduction Method, in: Proceedings of the 22nd IMAC, 2004.
[13] S. Donders, B. Pluymers, P. Ragnarsson, R. Hadjit, W. Desmet, The wave-based substructuring approach for the efficient description of interface dynamics in substructuring, Journal of Sound and Vibration 329 (2010) 1062–1080.
[14] S. N. Voormeeren, Dynamic Substructuring Methodologies for Integrated Dynamic Analysis of Wind Turbines, Ph.D. thesis, Delft University of Technology, Delft, 2012. URL: http://resolver.tudelft.nl/uuid:f45f0548-d5ec-46aa-be7e-7f1c2b57590d.
[15] M. P. Castanier, Y.-C. Tan, C. Pierre, Characteristic Constraint Modes for Component Mode Synthesis, AIAA Journal 39 (2001) 1182–1187.
[16] K. Brahmi, N. Bouhaddi, R. Fillod, Reduction of Junction Degrees of Freedom in Certain Methods of Dynamic Substructure Synthesis, in: Proceedings of the 13th IMAC, 1995.
[17] M. Geradin, D. J. Rixen, Mechanical Vibrations: Theory and Application to Structural Dynamics, 3rd edition ed., Wiley, 2015.
[18] Roy R. Craig Jr., A. J. Kurdila, Fundamentals of Structural Dynamics, 2nd edition ed., Wiley, Hoboken, N.J, 2006. 00360.
[19] R. J. Allemang, D. L. Brown, A correlation coefficient for modal vector analysis, in: Proceedings of the 1st IMAC, 1982.